Carbon Monoxide Modulates Apoptosis by Reinforcing Oxidative Metabolism in Astrocytes

ROLE OF Bcl-2*[S]

Ana S. Almeida[‡§], **Cláudia S. F. Queiroga**[‡§¶], **Marcos F. Q. Sousa**[‡], **Paula M. Alves**[‡¶], and **Helena L. A. Vieira**[‡§¶1]

From the [‡]*Instituto de Biologia Experimental e Tecnológica, Apartado 12, 2781-901 Oeiras, Portugal,* [¶]*Instituto de Tecnologia Química e Biológica, Universidade Nova de Lisboa, Apt 127, 2781-901 Oeiras, Portugal, and* [§]*Chronic Diseases Research Center, Faculdade de Ciências Médicas, Universidade Nova de Lisboa, 1169-056 Lisboa, Portugal*

Background: Low doses of carbon monoxide (CO) prevent apoptosis in several cell models, including astrocytes.
Results: CO improves cytochrome *c* oxidase (COX) activity and induces mitochondrial biogenesis. Bcl-2 expression and interaction with COX is involved in CO signaling.
Conclusion: CO stimulates oxidative phosphorylation, improves metabolism, and prevents astrocytic apoptosis.
Significance: Metabolism modulation can be a potential strategy against cerebral ischemia.

Modulation of cerebral cell metabolism for improving the outcome of hypoxia-ischemia and reperfusion is a strategy yet to be explored. Because carbon monoxide (CO) is known to prevent cerebral cell death; herein the role of CO in the modulation of astrocytic metabolism, in particular, at the level of mitochondria was investigated. Low concentrations of CO partially inhibited oxidative stress-induced apoptosis in astrocytes, by preventing caspase-3 activation, mitochondrial potential depolarization, and plasmatic membrane permeability. CO exposure enhanced intracellular ATP generation, which was accompanied by an increase on specific oxygen consumption, a decrease on lactate production, and a reduction of glucose use, indicating an improvement of oxidative phosphorylation. Accordingly, CO increased cytochrome *c* oxidase (COX) enzymatic specific activity and stimulated mitochondrial biogenesis. In astrocytes, COX interacts with Bcl-2, which was verified by immunoprecipitation; this interaction is superior after 24 h of CO treatment. Furthermore, CO enhanced Bcl-2 expression in astrocytes. By silencing Bcl-2 expression with siRNA transfection, CO effects in astrocytes were prevented, namely: (i) inhibition of apoptosis, (ii) increase on ATP generation, (iii) stimulation of COX activity, and (iv) mitochondrial biogenesis. Thus, Bcl-2 expression is crucial for CO modulation of oxidative metabolism and for confering cytoprotection. In conclusion, CO protects astrocytes against oxidative stress-induced apoptosis by improving metabolism functioning, particularly mitochondrial oxidative phosphorylation.

Proposing carbon monoxide (CO) as a therapeutic molecule is counterintuitive at first glance because for many decades, it has been seen primarily as a toxic gas and "silent killer" due to its high affinity for hemoglobin. However, CO has been identified as an endogenous product of heme degradation by heme oxygenase activity. Furthermore, CO is recognized largely as a homeostatic molecule, modulating inflammation, apoptosis, and proliferation (1, 2). Three main areas of potential therapeutic applications have been studied extensively: cardiovascular diseases, inflammatory disorders, and organ transplantation (1, 3).

The cytoprotective and, in particular, anti-apoptotic role of CO is described widely in the airways and cardiovascular system (4). The anti-apoptotic protein Bcl-2 also seems to be involved in CO-induced cytoprotection. CO-stimulated Bcl-2 expression has conferred protection in a lung model of ischemia reperfusion (5), whereas overexpression of heme oxygenase 1 was neuroprotective in a model of permanent middle cerebral artery occlusion in transgenic mice by increasing Bcl-2 levels in neurons (6). In the central nervous system (CNS), low concentrations of CO suppressed neuroinflammation in a model of multiple sclerosis (experimental autoimmune encephalomyelitis) (7) and induced vasodilatation in a model of epileptic seizures in newborn piglets (8). In primary cultures of neurons and astrocytes, CO induced preconditioning by *de novo* protein synthesis and by post-translational protein modification, respectively, preventing apoptosis (9, 10). In an adult model of cerebral ischemia, brain lesion was less marked in CO-pretreated animals (11, 12).

However, the association between CO-induced metabolic changes and its cytoprotective role remains unclear. In hepatocytes, ATP production is stimulated by increasing enzymatic activity of heme oxygenase or by administrating of CO (13, 14), which enhances resistance against hepatic apoptosis. On the other hand, CO has been shown to target and inhibit cytochrome *c* oxidase, generating ROS,[2] which are important sig-

naling molecules for CO action (15–18). In cardiomyocytes, CO triggers mitochondrial biogenesis in a ROS-dependent mode (19) and prevents murine doxorubicin cardiomyopathy (20). Still, ROS (in particular hydrogen peroxide and anion superoxide) are crucial intracellular signaling molecules for CO to prevent apoptosis in astrocytic and neuronal primary cultures (9, 10).

Hypoxia-ischemia and reperfusion, due to stroke in adults and to perinatal complications in newborns, are the main cause of brain damage. Cerebral damage is a result of oxygen and tissue energy depletion, leading to acidosis, inflammation, glutamate excitotoxicity, and generation of ROS (21, 22). Stimulation of angiogenesis is the single strategy based on improving metabolism for treating cerebral hypoxia-ischemia and reperfusion (21). Thus, novel strategies targeting cellular metabolic performance represent a window of opportunity for addressing and improving brain ischemia outcome. Furthermore, astrocytes are the most metabolic active cells in the CNS and are involved in brain structural support, repair after trauma, and maintenance of normal neuronal transmission and metabolism. Herein, the role of CO in astrocytic metabolism to confer cytoprotection and prevent damage in a model of hypoxia-ischemia and reperfusion is explored. The hypothesis lies on an enhancement of oxidative metabolism by CO via modulation of cytochrome *c* oxidase activity and mitochondrial biogenesis; both events are dependent on Bcl-2 expression.

EXPERIMENTAL PROCEDURES

Materials—All of the chemicals were of analytical grade and were obtained from Sigma-Aldrich unless stated otherwise. Plastic tissue culture dishes were from Nunc (Roskilde, Denmark); fetal bovine serum, penicillin/streptomycin solution, and Dulbecco's minimum essential medium were obtained from Invitrogen; and Wistar rats were purchased from Instituto de Higiene e Medicina Tropical (Lisboa, Portugal).

Cell Culture in Monolayer—Primary cultures of astrocytes were prepared from 2-day-old rat cortex as described (23, 24). Briefly, cerebral hemispheres were carefully freed of the meninges, washed in ice-cold PBS, and disrupted mechanically. Single-cell suspensions were plated in T-flasks (three hemispheres/175 cm2) in Dulbecco's minimum essential medium supplemented with 10% (v/v) FBS (heat-inactivated), 100 units/ml penicillin/streptomycin solution, and glucose (to obtain a final concentration of 10 mM). Cells were maintained in a humidified atmosphere of 7% CO_2 at 37 °C. After 8 days, the phase dark cells growing on the astrocytic cell layer were separated by vigorous shaking and removed. The remaining astrocytes were detached by mild trypsinization using trypsin/EDTA (0.25%, w/v) and subcultured in T-flasks for another 2 weeks. Growth medium was changed twice a week.

Cell Culture in Bioreactor—After 3 weeks of astrocytes isolation in T-flasks, cells were harvested by mild trypsinization and immobilized in Cytodex 3 microcarriers (3 g/liter, GE Healthcare) using a cell inoculum of $\sim 0.35 \times 10^6$ cell/ml. Immobilized cells were initially cultivated in spinner flask at 100 rpm, in an incubator at 37 °C with 7% CO_2 in air. 50% of the culture volume was exchanged twice a week, and cells were allowed to grow until reach confluence, prior to the experiments in biore-

actor, for assessing glucose consumption, lactate production, and specific oxygen consumption. To carry out the assays in bioreactor, fully controlled cell culture environment was guaranteed by the use of commercially available bioreactors (Biostat Q-Plus, Sartorius-Stedim, Germany) with 250 ml of working volume and equipped with a three-blade impeller. Partial pressure of oxygen, pH, and temperature were monitored using adequate probes (both from Mettler-Toledo, Urdorf, Switzerland). Partial pressure of oxygen was maintained constant at 30% of air saturation via surface aeration with a mixture of N_2. pH and temperature were controlled at 7.2 and 37 °C by CO_2 injection and water recirculation in the vessel jacket, respectively. Stirring was set to 100 rpm. For bioreactor control and data acquisition, MFCS/Win software (version 2.1) was used (Sartorius AG).

Measurement of Oxygen-specific Consumption (qO_2)—Oxygen uptake rate (OUR) was assessed continuously during the culture by using Equation 1,

$$OUR = kLa \times (C^* - C) \qquad \text{(Eq. 1)}$$

where *kLa* is the mass transfer coefficient calculated previously for the used culture conditions (data not shown) as described in Ref. 25; C^* is saturated oxygen concentration, and *C* is oxygen concentration in solution.

Then, the qO_2 value was determined using Equation 2.

$$qO_2 = OUR/X_v \qquad \text{(Eq. 2)}$$

OUR and X_v (viable cell concentration) values used for qO_2 correspond to the same specific time point of the culture.

Lactate/Glucose Ratio—Total glucose and lactate concentrations in the culture supernatant (from bioreactor system) were determined with automated enzymatic assays (YSI 7100 Multiparameter Bioanalytical System; Dayton, OH). The rate between lactate production and glucose consumption was obtained by linear regression of the metabolites concentrations.

siRNA Transfection—Bcl-2 expression was silenced by Bcl-2 coding siRNA transfection according to the manufacturer's instructions (Invitrogen). Astrocytes at 40% of confluence were transfected using Lipofectamine$^{\text{TM}}$ RNAiMAX and Opti-MEM® medium (Invitrogen); for 2, 3.9, or 79 cm^2 of astrocytic culture area 6, 12, or 237 pmol of siRNA were used, respectively. At room temperature, siRNA and culture medium were mixed gently with Lipofectamine for forming liposomes, and then astrocytes were transfected in the absence of antibiotics. 24, 48, and 72 h after transfection Bcl-2 expression was assessed by Western blot assay, silencing was more efficient between 24 and 48 h, and then Bcl-2 silenced astrocytes were used in this time frame.

Isolation of Non-synaptic Mitochondria from Cortex—Enriched fractions of non-synaptic mitochondria were isolated from 300–350-g male Wistar adult rats according to Refs. 26 and 27. Briefly, the cortex was removed and washed in a ice-cold isolation buffer containing 225 mM manitol, 75 mM sucrose, 1 mM EGTA, and 5 mM HEPES, pH 7.4. The tissue was minced with scissors and homogenized manually with Potter-Elvehjem in isolation buffer. The homogenate was centrifuged at 1300 × *g* for 3 min, and the resuspended pellet was recentri-

fuged at 1300 × *g* for 3 min. Both supernatants were pooled together and centrifuged at 21,200 × *g* for 10 min. The remaining pellet was resuspended in 3.5 ml of 15% Percoll solution and layered into centrifuge tubes containing a preformed two-step discontinuous density gradient consisting of 3.7 ml of 24% Percoll on top of 1.7 ml of 40% Percoll. The gradient was centrifuged at 31,700 × *g* for 9 min. The mitochondrial fraction, located between the layers of 24 and 40% Percoll, was removed, diluted 1:8 in isolation buffer, and centrifuged at 16,700 × *g* for 10 min. The pellet was resuspended in 10 ml of isolation buffer containing 5 mg/ml bovine serum albumin (to remove lipids) and centrifuged at 6,800 × *g* for 10 min. The mitochondrial pellet was resuspended in 100 μl of isolation buffer, and the total amount of protein was quantified using a BCA assay (Pierce). All of the steps were carried out at 4 °C. All isolated mitochondria analyses were performed on modified brain buffer (26) containing 125 mM KCl, 2 mM K_2HPO_4, 1 mM $MgCl_2$, 15 M EGTA, 20 mM Tris, 5 mM glutamate, and 5 mM malate, pH 7.3, unless stated otherwise. All CO treatment in isolated mitochondria was performed with a final concentration of 10 μM for 5, 30, and 60 min at 37 °C.

Preparation of CO Solutions—Fresh stock solutions of CO gas were prepared each day and sealed carefully. PBS was saturated by bubbling 100% of CO gas for 30 min to produce $10e^{-3}$ M stock solution. The concentration of CO in solution was determined spectrophotometrically by measuring the conversion of deoxymyoglobin to carbon monoxymyoglobin as described previously (40). 100% CO was purchased as compressed gas (Linde, Germany).

Assessment of Apoptosis-associated Parameters by Flow Cytometry—To detect apoptosis induced by *tert*-butylhydroperoxide (*t*-BHP), cell samples were collected by trypsinization, and cells were gated by the forward and side scatter. Two dyes were used: 3,3′-dihexyloxacarbocyanine iodide ($DiOC_6(3)$; 20 nM) (Invitrogen) to quantify the mitochondrial transmembrane potential ($\Delta\Psi$m) and propidium iodide (1 μg/ml) (Invitrogen) to determine cell viability, based on plasma membrane integrity. A flow cytometer (Partec) was used to analyze apoptosis-associated parameters. This cytometer contains a blue solid state laser (488 nm) with FL1 green fluorescence channel for $DiOC_6$ (3) at 530 nm and a FL3 red fluorescence channel for propidium iodide detection at 650 nm. The acquisition and analysis of the results were performed with FlowMax® software (Partec).

Immunoprecipitation—100 μg of mitochondrial protein (isolated from astrocytes or from rat cortex) were incubated in 100 μl of homogenization buffer containing 0.5% of Triton X-100 in the presence of 30 μl of COX (Santa Cruz Biotechnology; 200 μg/ml) for 90 min at 37 °C, followed by immunoprecipitation with 15 μl of protein A/G PLUS-agarose beads (Santa Cruz Biotechnology) during 30 min at 37 °C. After 10 min of 10,000 × *g* centrifugation, supernatant was discarded, and pellet was washed four times with PBS. Proteins attached to the beads were solubilized by Laemmli buffer for further Western blot analysis.

Immunoblotting—Several samples (from cell extracts, mitochondria, or immunoprecipitated protein) were separated under reducing electrophoresis on a 1 mm of NuPAGE® Novex Bis-Tris gel (Invitrogen) and transferred to a nitrocellulose membrane (Hybond™-C extra, Amersham Biosciences). Caspase-3 or Bcl-2 protein was stained with α-active caspase-3 (Sigma C8487) or α-Bcl-2 (Santa Cruz Biotechnology) at 1/1000 dilution for 2 h at room temperature. Blots were developed using the ECL (enhanced chemiluminescence) detection system after incubation with HRP-labeled anti-mouse IgG antibody (Amersham Biosciences Bioscience), 1/5000, 1 h of room temperature incubation. These experiments have been repeated three times, with similar results.

Mitochondrion Isolation from Primary Culture of Astrocytes—Primary cultures of astrocytes were pretreated 3 and 24 h with CO (final concentration of 50 μM). Cells were washed with ice-cold PBS and collected by trypsinization. The samples were centrifuged at 200 × *g* for 10 min, and cells were washed in PBS by centrifugation at 200 × *g* for 10 min. The supernatant was discarded, and the pellet (cells) was incubated in 3.5 ml of hypotonic buffer (0.15 mM $MgCl_2$, 10 mM KCl, 10 mM Tris-HCl, pH 7.6) at 4 °C for 5 min. After the addition of an equal volume of homogenization buffer (0.15 mM $MgCl_2$, 10 mM KCl, 10 mM Tris-HCl, 0.4 mM phenylmethylsulfonyl fluoride, 250 mM saccharose, pH 7.6) twice concentrated, samples were manually homogenized with a Dounce Potter homogenizer. Cell extracts were centrifuged at 900 × *g* for 10 min, followed by supernatant centrifugation at 10,000 × *g* for 10 min. The mitochondrial pellet was resuspended in 100 μl of homogenization buffer, and the total amount of protein was quantified using BCA assay (Pierce). All of the steps were carried out at 4 °C.

ATP Quantification—Intracellular ATP of primary astrocytes pretreated with CO (final concentration of 50 μM) was quantified using the ATPlite 1 step Luminescence ATP detection assay system (PerkinElmer Life Sciences), according to the manufacturer's instructions.

Polymerase Chain Reaction—Genomic DNA was extracted from astrocytes using the High Pure PCR Template preparation kit (Roche Diagnostics, Mannheim, Germany). PCR was performed using specific forward and reverse primers designed for the mitochondrial cytochrome *b* gene (5′-CAT CAG TCA CCC ACA TCT GC-3′ and 5′-GGT TAG CGG GTG TAT AAT TG-3′) and for the GAPDH gene (5′-CCT TCA TTG ACC TCA ACT ACA T-3′ and 5′-CCA AAG TTG TCA TGG ATG ACC-3′), respectively. Fast Start DNA Master Plus SYBR Green I (Roche Diagnostics) was used with the experimental run protocol: denaturation program was 95 °C for 10 min, followed by 45 cycles of 95 °C for 15″, 60 °C for 6′′ and 72 °C for 20′′. For evaluation of Bcl-2 expression, mRNA was extracted from astrocytes using High Pure RNA isolation kit (Roche Diagnostics), and cDNA synthesis was performed using the Transcriptor High Fidelity cDNA synthesis kit (Roche Diagnostics). PCR was performed using specific forward and reverse primers designed for the Bcl-2 gene (5′-GGTGGAGGAACTCTTCAGGG-3′ and 5′-GAGACAGCCAGGAGAAATCA-3′) and for the cyclophilin A gene (5′-ATGGCAAATGCTGGACC-AAA-3′ and 5′-GCCTTCTTTCACCTTCCCAAA-3′), respectively. Fast Start DNA Master Plus SYBR Green I (Roche Diagnostics) was used with the experimental run protocol: denaturation program was 95 °C for 10 min, followed by 45 cycles of 95 °C for 15 min, 66 °C for 10 min and 72 °C for 15 min.
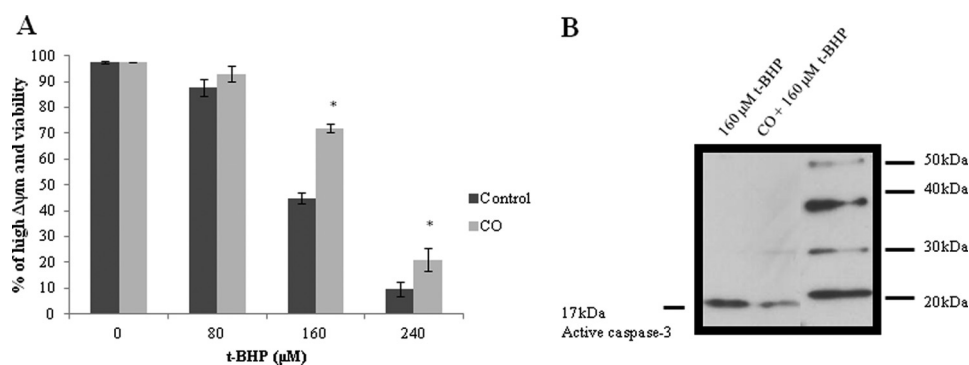
FIGURE 1. **Carbon monoxide confers protection against apoptosis.** Primary cultures of astrocytes cultured in 24-well plates were pretreated with 50 μM of CO for 3 h, following apoptosis induction by 20 h of exposure to the pro-oxidant, t-BHP (from 0 to 240 μM). The apoptotic hallmarks were assessed by flow cytometry. In A, the percentage of cells presenting high mitochondrial potential (detected by $DiOC_6(3)$) and containing intact plasma membrane (assessed with propidium iodide) is presented. All values are mean $\pm$ S.D. ($n = 4$). *, $p < 0.05$ compared with control and CO-treated cells for each concentration of t-BHP. B, representative picture of immunodetection of caspase-3 activation by its cleavage into the 17-kDa fraction. The first line corresponds to astrocytes treated with t-BHP at 160 μM (20 h); the second line astrocytes pretreated with 50 μM of CO (3 h) followed by t-BHP induction of apoptosis.

Cytochrome c Oxidase Activity—To assess CO early effect in COX activity (5 min, 30 min, and 1 h), 100 μg of non-synaptic mitochondria from cortex were treated with 10 μM of CO followed by COX activity measurements. For late effect, mitochondria from pretreated astrocytes were isolated, and then 100 μg of mitochondria were used to quantify COX enzymatic activity. In both cases, COX activity was quantified using the cytochrome c oxidase assay kit (Sigma-Aldrich), according to the manufacturer's instructions.

Statistical Analyses—The data concerning astrocytic culture were carried out at least in three independent preparations (cell isolation). All data related to isolated non-synaptic mitochondria were done in triplicate from at least three independent animals. For Western blotting, a representative image of three independent assays is shown. All values are mean $\pm$ S.D. ($n \geq 3$). Error bars, corresponding to S.D., are shown in the figures. Statistical comparisons were performed using analysis of variance: single factor with replication, with $p < 0.05$ ($n \geq 3$). $p < 0.05$ means that samples are significantly different at a confidence level of 95%.

RESULTS

Carbon Monoxide Prevents Apoptosis and Increases Intracellular ATP—3 h prior to apoptosis induction, primary culture of astrocytes was pretreated with CO-saturated solutions at a final concentration of 50 μM. Then, astrocytes were challenged with the pro-oxidant *tert*-butylhydroperoxide (80 to 240 μM) during 20 h to trigger apoptosis by oxidative stress. The assessed hallmarks of apoptosis were dissipation of mitochondrial membrane potential ($\Delta\psi m$), caspase-3 activation and plasma membrane permeabilization, a late event on the apoptotic process (also called secondary necrosis). Dissipation of $\Delta\psi m$ (quantified by $DiOC_6(3)$) and plasma membrane permeabilization (detected by iodide propidium fluorescence) were measured by flow cytometry. The presence of CO partially prevents dissipation of $\Delta\psi m$ and permeabilization of plasma membrane (Fig. 1A). Caspase-3 activation was assessed by Western blot assay, in CO-treated astrocytic culture, there was less activated caspase-3 (Fig. 1B). Thus, in accordance to our previous work (9), CO prevents astrocytic apoptosis.
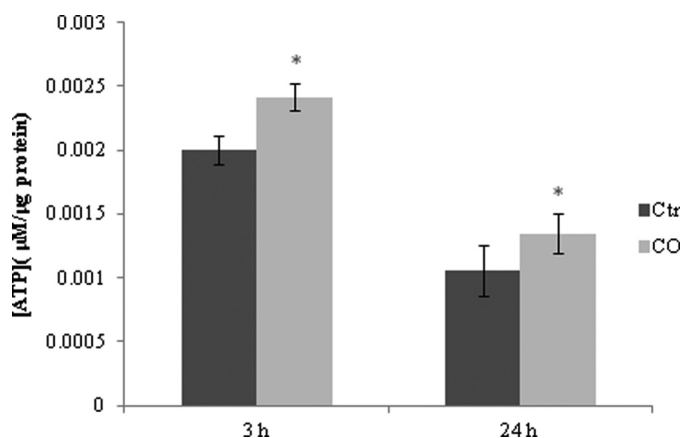

FIGURE 2. **CO increases ATP generation in astrocytes.** Astrocytes were treated with 50 μM of CO for 3 and 24 h, followed by ATP assessment. ATP concentration is represented per μg of protein from cellular extract. All values are mean $\pm$ S.D. ($n = 3$). *, $p < 0.05$ compared with control and CO-treated cells for 3 and 24 h. *Ctr*, control.

It is worthy of note that upon opening the sealed vial of CO-saturated solution, CO diffuses out quickly from the cell culture system; after 30 min, >50% is already lost in the atmosphere.[3] Additionally, up to 48 h after CO treatment, astrocytes still present increased resistance against cell death (supplemental Fig. S1). Hence, CO action might occur by activating endogenous mechanisms and by altering gene expression.

In addition, the effect of CO on astrocytes does not appear to be limited to shifting cell death signaling pathways, but this gaseous transmitter also changes cell metabolism. Intracellular ATP concentration is higher at 3 and 24 h after CO treatment than in non-treated astrocytes (Fig. 2). Thus, cellular metabolism alterations seem to be involved in prevention of astrocytic apoptosis by CO via an increase of cellular energetic supply.

Carbon Monoxide Improves Oxidative Metabolism—Glycolysis comprises a series of biochemical reactions by which glucose is converted into pyruvate, which may be further converted into metabolic products such as lactate or enter into a tricarboxylic acid (TCA) cycle. To disclose the metabolic path-

---

[3] J. Seixas, personal communication.

TABLE 1
Metabolic Hallmarks

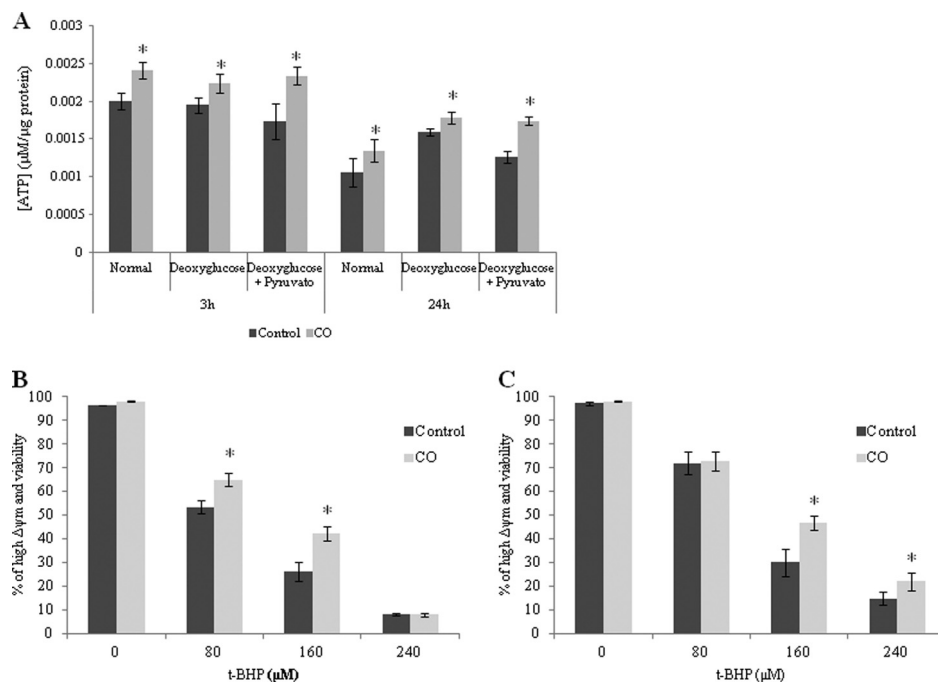|	Glucose consumption	Lactate production	Lac/Glc	qO$_2$
	pmol/h/cell ± *S.D.*	*pmol/h/cell* ± *S.D.*		*μmol/10^6 cell/h* ± *S.D.*
No treatment	0.2612 ± 0.0022	0.4460 ± 0.0003	1.708	0.142 ± 0.006
CO treatment (50 μM)	0.2923 ± 0.0337	0.3831 ± 0.0426	1.311	0.170 ± 0.0130

FIGURE 3. **Effect of CO on ATP production and protection against cell death under glycolysis-limiting conditions.** Astrocytes were cultured in glucose-free medium complemented with 2 mM deoxyglucose (for inhibiting small amounts of glucose presented in FBS) (*A* and *B*) and glucose-free medium with deoxyglucose and 2 mM pyruvate (for directly feeding the TCA cycle) (*A* and *C*) for 2 h. *A*, astrocytes were treated with 50 μM CO for 3 and 24 h, followed by ATP assessment. ATP concentration is represented per μg of protein from cellular extract. All values are mean ± S.D. (*n* = 3). *, *p* < 0.05 compared with control and CO-treated cells for 3 and 24 h, under normal conditions and glycolysis-limiting conditions. After culturing astrocytes in glucose-free medium complemented with 2 mM deoxyglucose (*B*) and glucose-free medium with deoxyglucose and 2 mM pyruvate (*C*) for 2 h, 50 μM CO was added for 3 h, followed by cell death induction with *t*-BHP (0 to 240 μM). The apoptotic hallmarks were assessed by flow cytometry as in Fig. 1. All values are mean ± S.D. (*n* = 3). *, *p* < 0.05 compared with control and CO-treated cells for each concentration of *t*-BHP.

way involved in the CO-induced ATP enhance and to follow whether the cellular metabolic shift is further glycolytic or oxidative, the levels of lactate production and glucose consumption were monitored. Specific rates of glucose consumption or lactate production (μmol h^{-1} per cell) were calculated throughout 36 h after CO treatment (50 μM) in astrocytic cultures performed in bioreactors, and data are summarized in Table 1. Upon CO addition, the lactate production/glucose consumption ratio decreased, meaning that higher amounts of pyruvate entered and were metabolized by the TCA cycle (28). Additionally, the specific rate of oxygen consumption (qO$_2$) was calculated in the presence of CO in astrocytes cultured for 36 h in the bioreactor system. CO treatment increases oxygen consumption by astrocytes in ~20% (Table 1). Given that CO decreases the lactate production/glucose consumption ratio and increases specific oxygen consumption, the CO-induced enhance in ATP production appears to be derived from oxidative phosphorylation improvement.

Furthermore, to verify the importance of glycolytic metabolism in astrocytes after CO treatment, glycolysis was limited by two different strategies: (i) using glucose-free medium in the presence of deoxyglucose (which competes with the remaining glucose from the serum) or the (ii) same strategy as mentioned previously, with the addition of pyruvate to reinforce the TCA cycle and oxidative phosphorylation. After 2 h of astrocytic culture under glycolysis-limiting conditions, CO was added to the culture medium. In both strategies, CO treatment still increased the levels of ATP in astrocytes after 3 and 24 h (Fig. 3*A*). Thus, CO-induced ATP enhance was not due to an improvement on glycolytic metabolism. Additionally, glycolysis limitation did not prevent CO-triggered cytoprotection in astrocytes because there is inhibition of astrocytic apoptosis by CO when glucose is not available (Fig. 3, *B* and *C*).

The effect of CO on COX activity was measured to assess the influence of this gaseous transmitter on oxidative phosphorylation. Two distinct approaches were followed. First, non-synaptic mitochondria isolated from rat cerebral cortex were treated with CO at 10 μM, and COX activity was measured at 5, 30, and 60 min after treatment. Although being a less physiological approach, this strategy allows the assessment of the mitochondrial early response to CO (in particular at the level of COX activity). Immediately after CO addition (5 min), COX activity decreases slightly (Fig. 4*A*), which is in accordance with Refs. 16–18 and 29). Although a small effect, it is statistically significant. After 30 and 60 min of CO treatment, this inhibition is reverted (Fig. 4*A*).
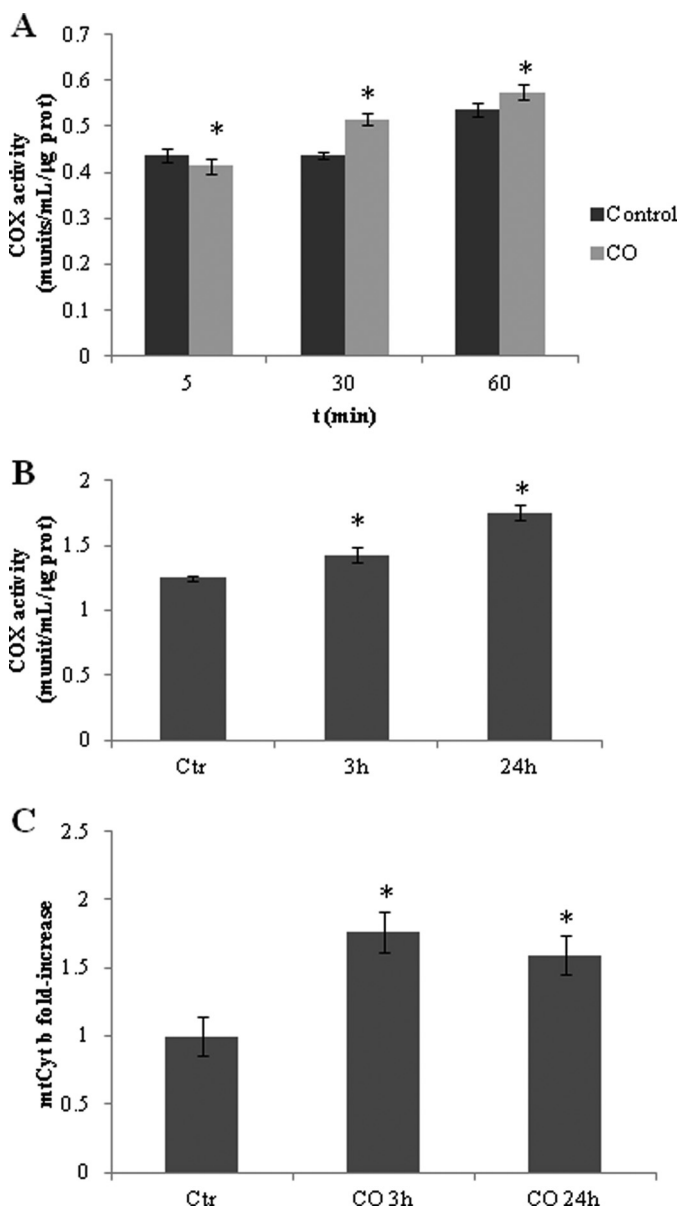
FIGURE 4. **Effect of CO on cytochrome *c* oxidase activity and mitochondria biogenesis.** *A*, non-synaptic mitochondria were isolated from rat cortex, 100 μg were treated with 10 μM CO, and COX enzymatic activity was assessed at 5, 30, and 60 min. All values are mean $\pm$ S.D. ($n = 3$). *, $p < 0.05$ compared with control and CO-treated cells for 5, 30, and 60 min. *B*, astrocytes were treated with 50 μM CO for 3 and 24 h, followed by mitochondria isolation (100 μg) and COX activity measurements. All values are mean $\pm$ S.D. ($n = 3$). *, $p < 0.05$ compared with control and CO-treated cells for 3 and 24 h. *C*, astrocytes were treated with 50 μM of CO for 3 and 24 h, followed by DNA extraction for measuring mitochondrial cytochrome *b* (*mtCyt b*) gene to assess mitochondrial DNA amount, which is represented by fold increase when compared with control without CO treatment. All values are mean $\pm$ S.D. ($n = 4$). *, $p < 0.05$ compared with control and CO-treated cells for 3 and 24 h. *munits*, milliunits; *prot*, protein; *Ctr*, control.

In a second strategy, astrocytes were treated with 50 μM of CO for 3 or 24 h, followed by mitochondria isolation for COX activity assessment. In this more physiological approach, CO increased specific COX activity at 3 and 24 h (Fig. 4*B*). Therefore, COX activity presents a two-step response to low concentrations of CO: in the first minutes, CO slightly inhibits its enzymatic activity in isolated mitochondria, whereas after 30 or 60 min of CO treatment in the case of isolated mitochondria, and

3 or 24 h when gas treatment is done in whole intact astrocytes, low concentrations of CO appear to improve COX activity. This two-step response is in accordance to our previous work in isolated liver mitochondria, showing that CO transiently inhibited COX activity up to 10 min after treatment, followed by an enzymatic activity improvement at 30 min (30).

In addition to COX activity assays, the influence of CO treatment on cellular mitochondrial population also was assessed. Quantitative real-time PCR was used to quantify mitochondrial coding gene for cytochrome *b*, which estimates mitochondrial biogenesis. Indeed, 3 h of CO treatment induced a 50% increase on mitochondrial cytochrome *b* DNA in astrocytes, meaning that CO stimulates mitochondrial DNA replication and, consequently, mitochondrial biogenesis. At 24 h, there is a slight decrease on the amount of cytochrome *b* DNA (Fig. 4*C*). These data are in accordance with Suliman and co-workers (19, 20), who have shown that in cardiomyocytes CO induces mitochondrial biogenesis in a ROS-dependent manner. Taken together, CO improves oxidative cell metabolism and increases ATP production by two distinct mechanisms: accelerating specific enzymatic activity of COX and increasing cellular mitochondrial population.

Role of Bcl-2 in Oxidative Phosphorylation—CO modulates the expression of the anti-apoptotic protein Bcl-2, preventing cell death in a lung model (6, 5). On the other hand, Chen and co-workers (31, 32) have demonstrated that Bcl-2 promotes survival of cancer cells by elevating mitochondrial respiration through the direct interaction with COX and improvement of its activity. Thus, we hypothesized that CO could also increase Bcl-2 expression in astrocytes and that Bcl-2 could be involved on CO-triggered improvement of COX activity. CO modulation of Bcl-2 expression was evaluated by reverse transcriptase quantitative PCR. Astrocytes were treated with 50 μM of CO for 3 and 24 h, and then total mRNA was purified, and the corresponding cDNA was synthesized by reverse transcriptase activity and quantified by real-time PCR. CO induced an increased on Bcl-2 mRNA (Fig. 5*A*). To assess the physical interaction of COX and Bcl-2 upon CO action, immunoprecipitation assays were conducted. Purified mitochondria from control astrocytes or from CO-treated astrocytes for 3 and 24 h were incubated with α-COX to immunoprecipitate the attached proteins to cytochrome *c* oxidase, followed by immunodetection of Bcl-2 by Western blot assay. The presence of CO augments the interaction between Bcl-2 and COX after 24 h of CO treatment (Fig. 5*B*); however, after 3 h the increase in protein-protein interaction is not significant. Therefore, the augmentation of Bcl-2-COX interaction might occur due to an increase on Bcl-2 expression. Taken together, Bcl-2 is involved in CO-stimulated cytochrome *c* oxidase activity.

To validate this hypothesis, Bcl-2 expression was silenced transiently by cell transfection with siRNA coding for Bcl-2. Silencing was confirmed by protein expression analysis via Western blot assay 24 and 48 h after transfection (supplemental Fig. S2). Silencing of Bcl-2 expression prevented the cytoprotective effect of CO, which was demonstrated by flow cytometry analysis upon oxidative stress induction. CO pretreatment was not able to inhibit plasma membrane permeabilization (detected by iodide propidium fluorescence) or dissipation of mitochondrial membrane potential, $\Delta\psi$m, (quantified by
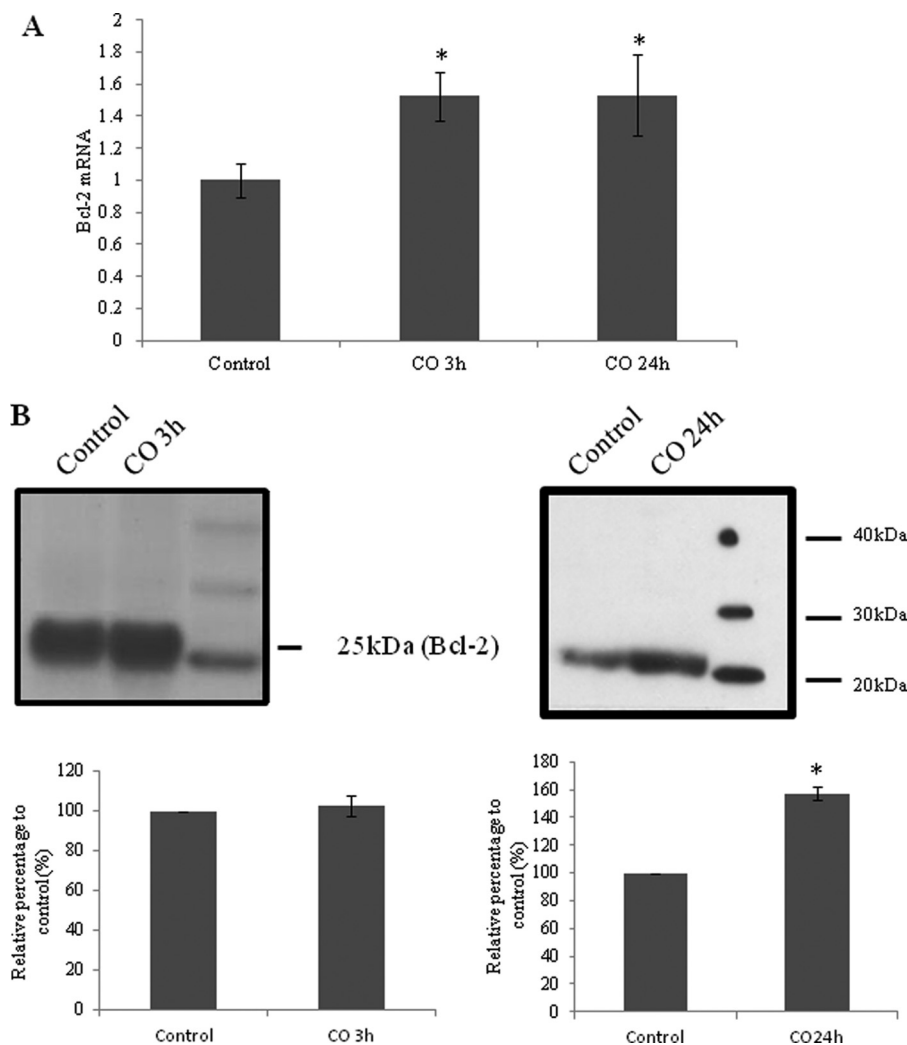
FIGURE 5. **Role of CO in expression of Bcl-2 and Bcl-2-COX interaction.** *A*, mRNA of Bcl-2 was quantified at 3 and 24 h of CO treatment at 50 μM. Values are represented in comparison with control astrocytes without CO treatment. All values are mean $\pm$ S.D. ($n = 3$). *, $p < 0.05$ compared with control and CO-treated cells for 3 and 24 h. *B*, COX was immunoprecipitated in mitochondria isolated from astrocytes treated with CO at 50 μM for 3 and 24 h, and Bcl-2 was immunodetected by Western blot from the immunoprecipitated proteins. The area and intensity of bands were quantified by densitometry analysis (GraphPad Prism 4) and are presented as relative percentage to the positive control (100%). All values are mean $\pm$ S.D. ($n = 3$). *, $p < 0.05$ compared with control and CO-treated cells for 24 h.

DiOC$_6$(3)) (Fig. 6*A*). Furthermore, whenever Bcl-2 expression is silenced CO did not prevent caspase-3 activation induced by pro-oxidant addition (Fig. 6*B*). The role of Bcl-2 is not limited to modulation of astrocytic apoptosis after oxidative stress challenge. Bcl-2 expression is also relevant for the following: (i) CO-induced ATP production, (ii) CO-increased COX activity, and (iii) CO-stimulated mitochondrial biogenesis. Indeed, Bcl-2 silencing prevented ATP generation enhancement by CO treatment (Fig. 6*C*). However, Bcl-2 expression is also crucial for CO to increase COX activity following gas exposition because by silencing Bcl-2, no increase on this enzymatic activity was observed (Fig. 6*D*). Finally, by silencing Bcl-2, CO did not stimulate any more mitochondria biogenesis after gas exposition (Fig. 6*E*). In conclusion, Bcl-2 expression and interaction with COX are crucial for CO improvement of oxidative phosphorylation.

DISCUSSION

Previously, we have demonstrated that CO confers protection against astrocytic cell death by directly acting on mito-

chondria and preventing mitochondrial membrane permeabilization, which is a key event in the intrinsic apoptotic pathway (9). The present work focuses on the role of CO in astrocytic metabolism modulation, in particular at mitochondrial level. Pretreatment of astrocytes with low doses of CO for 3 h (Fig. 1) or up to 48 h (supplemental Fig. S1) improved cellular response against stress and prevented apoptosis by preconditioning induction as published previously by the authors and others in several tissues (33, 9, 34, 10, 18).

To disclose the role of CO in astrocytic metabolism, the levels of ATP, the major cellular energy carrier, was assessed. Astrocytic ATP generation increases following CO treatment (Fig. 2). The two major pathways for ATP generation are glycolysis and oxidative phosphorylation. During 36 h after CO addition in an astrocytic culture, the ratio between lactate production and glucose consumption has decreased, whereas the oxygen consumption levels have increased, indicating that CO stimulated oxidative metabolism in contrast to glycolysis (Table 1). In addition, CO was able to increase ATP production
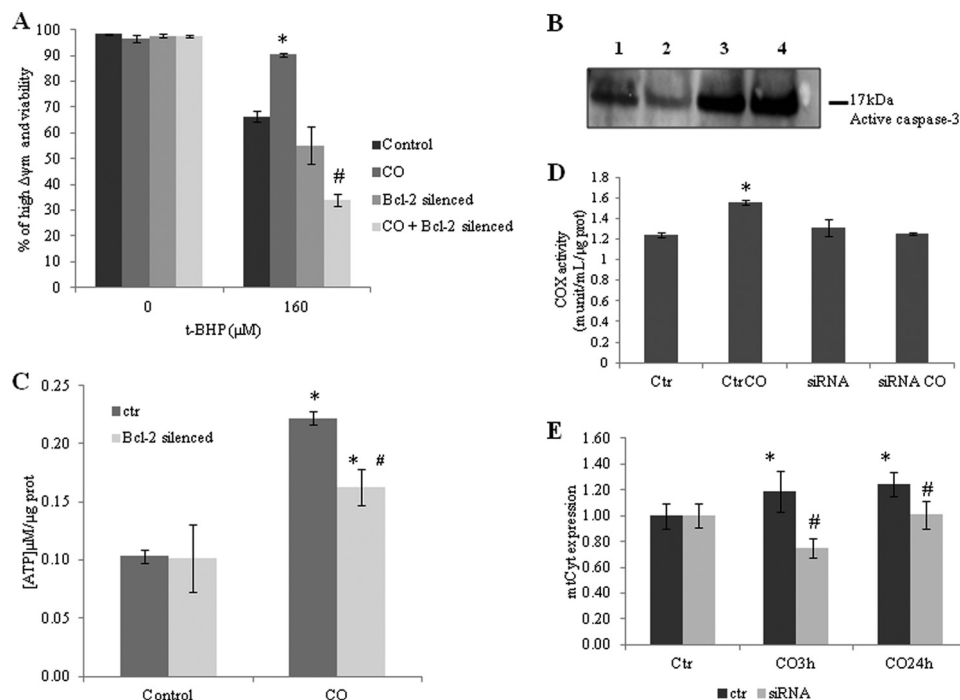
FIGURE 6. **Role of Bcl-2 in CO-induced astrocytic metabolism modulation.** Bcl-2 expression was silenced by siRNA transfection, and CO treatment was performed between 24 and 48 h after transfection, which is the period when gene silencing is optimal. Control and Bcl-2-silenced astrocytes were treated with CO for 3 h and challenged to death with 160 μM t-BHP for 20 h. A, cell death was assessed by flow cytometry (detected by DiOC$_6$(3) and propidium iodide). All values are mean ± S.D. ($n = 4$). *, $p < 0.05$ compared with control and CO-treated cells; #, $p < 0.05$ compared with Bcl-2 silenced astrocytes and CO-treated Bcl-2-silenced astrocytes. B, representative picture of immunodetection of caspase-3 activation by its cleavage into a 12-kDa fraction. Astrocytes were challenged to death with 160 μM t-BHP (*lane 1*), pretreated with CO (*lane 2*), Bcl-2 was silenced and astrocytes were treated with t-BHP (*lane 3*), and Bcl-2-silenced astrocytes pretreated with CO followed by t-BHP cell death induction (*lane 4*). C, Bcl-2 silenced and control astrocytes were treated with 50 μM of CO for 3 h, followed by ATP assessment. ATP concentration is represented per μg of protein from cellular extract. All values are mean ± S.D. ($n = 3$). *, $p < 0.05$ compared with non-treated and CO-treated cells for 3 h; #, $p < 0.05$ compared with Bcl-2-silenced astrocytes and control astrocytes, both treated with CO. D, 100 μg of mitochondria were isolated from control astrocytes and Bcl-2-silenced astrocytes, both treated or not with 50 μM CO for 24 h for COX activity measurement. All values are mean ± S.D. ($n = 5$). *, $p < 0.05$ compared with control and CO-treated cells. E, Bcl-2-silenced and control astrocytes were treated with 50 μM CO for 3 and 24 h, followed by DNA extraction for measuring mitochondrial cytochrome (*mtCyt*) b gene to assess mitochondrial DNA amount, which is represented by fold increase when compared with control without Bcl-2 silencing and CO treatment. All values are mean ± S.D. ($n = 4$). *, $p < 0.05$ compared with control and CO-treated cells; #, $p < 0.05$ compared with Bcl-2-silenced cells and non-silenced astrocytes for 3 and 24 h. *prot*, protein; *munit*, milliunits; *Ctr*, control.

and to prevent astrocytic cell death whenever glycolysis was inhibited (Fig. 3), suggesting that glycolysis is not affected by this gaseous transmitter.

Although in cancer cells, glycolysis promotes cytoprotection, in cerebral hypoxia-ischemia, glycolysis does not appear to present a similar function. In response to ischemia, glycolysis (which is necessary to maintain ATP levels under low levels of oxygen) leads to lactate accumulation and neural cell death by acidosis (21). The improvement of oxidative metabolism by restoring high energy stores (in particular ATP) without any glycolysis stimulation appears to confer neuroprotection in a cerebral preconditioning model (35). In myocardium ischemia, CO reduced glycolytic metabolism response (36). Furthermore, in macrophages, CO activated hypoxia-inducing factor-1 without increasing the rate of glycolysis (33). Additionally, Fukuda and colleagues have shown that activation of hypoxia-inducing factor-1 was involved in the regulation of cytochrome c oxidase subunits to optimize the efficiency of respiration in cancer cells (37). Taken together, from the present data and the literature, CO stimulates oxidative phosphorylation for preventing apoptosis in astrocytes.

In agreement with the previous data, CO also accelerates COX activity (Fig. 4, A and B). In a short time response (5 min), CO slightly decreased COX activity in isolated mitochondria,

which is in accordance with several published works (15–18), whereas after 30 min in isolated mitochondria and 3 and 24 h in the case of CO treatment of intact astrocytes, specific COX activity has increased (Fig. 4, A and B). Also in hepatic mitochondria, COX presented a two-phase response to low doses of CO: at 5 min, there was a decrease on its enzymatic activity, whereas after 30 min, the effect was inverted (30). One can speculate that CO role on COX activity might depend on two factors: (i) time response and (ii) gaseous transmitter concentration, giving rise to distinct enzymatic responses. Accordingly, CO also accelerated ATP/ADP translocase activity of ANT in non-synaptic mitochondria (9). Furthermore, Di Noia and co-workers (38) have demonstrated that heme oxygenase-1 overexpression enhanced renal oxidative phosphorylation by increasing mitochondrial transport carriers, in particular adenosine nucleotide translocase, and cytochrome c oxidase activity in experimental diabetes. In conclusion, previously published and present data indicate that CO improves mitochondrial respiratory chain. Although there is a clear effect of CO on COX activity, the molecular target of CO remains uncertain.

CO stimulation of oxidative metabolism is not limited to COX activity augmentation, but this gas also induced mitochondrial biogenesis in astrocytes (Fig. 4C). Suliman and co-workers (19) have demonstrated that CO stimulated mitochon-

drial biogenesis in cardiomyocytes. Herein, mitochondria rapidly respond to CO as mitochondrial DNA replication was detected after 3 h of CO treatment. In conclusion, CO stimulates oxidative phosphorylation by a double effect: (i) accelerates COX enzymatic activity and (ii) increases cellular mitochondrial population.

CO treatment enhanced the expression of the anti-apoptotic protein Bcl-2 (Fig. 5*A*). Furthermore, in cancer cells, Bcl-2 physically interacts with COX, increasing its enzymatic activity and oxidative phosphorylation, which induces a pro-oxidant state and cytoprotection (31, 32). In astrocytes, Bcl-2 also interacts with COX, and its interaction clearly increased at 24 h after CO treatment (Fig. 5*B*), which is in accordance with higher levels of Bcl-2 expression. In contrast, at 3 h of CO treatment, no increase on COX-Bcl-2 interaction was observed.

To validate the role of Bcl-2 in CO modulation of oxidative metabolism, astrocytes were transfected with siRNA (coding for Bcl-2) for transiently silencing this gene expression. It is not surprising that by silencing the anti-apoptotic protein Bcl-2, the extension of cell death was higher, and CO did not protect astrocytes against apoptosis (Fig. 6, *A* and *B*). The CO-induced metabolism modulation, such as increase on ATP generation, enhancement of COX activity, and stimulation of mitochondrial DNA replication (mitochondrial biogenesis), was at least partially prevented whenever Bcl-2 was silenced (Fig. 6, *C–E*). In conclusion, Bcl-2 expression is crucial for CO-triggered metabolism regulation and cytoprotection in astrocytes. It is worthy to note that Bcl-2 is important for CO mode of action not only when it is overexpressed but also when it is expressed under constitutive levels for two main reasons. First, modulation of cell metabolism by CO occurs at 3 h after gas exposition, indicating an early cell response that does not involve protein expression. Second, Bcl-2 silencing prevented CO metabolic effects on astrocytes at 3 h. Therefore, there are two types of cell response to CO: (i) early preconditioning (3 h) probably involving ROS signaling, post-translational protein modifications, or intracellular protein localization and (ii) late preconditioning (24 h), including changes in gene expression.

A preferential cellular target for CO is the mitochondrion. CO generates mitochondrial ROS for cell signaling (9, 10, 15–18), prevents mitochondrial membrane permeabilization (30, 9), and stimulates mitochondrial biogenesis (19, 20). Herein, CO acts at the mitochondrial level: it (i) improves oxidative metabolism, (ii) enhances mitochondrial population, (iii) modulates COX activity, (iv) increases cellular oxygen consumption, and (v) stimulates ATP production. However, the molecular target of CO is still unclear. The most accepted hypothesis is that CO can direct target COX inducing ROS generation at the level of complex III. CO-induced ROS can become toxic or signaling depending on its concentration. However, Iacono and co-workers (39) have proposed that CO can protect cell against oxidative stress by uncoupling mitochondria and decreasing ROS generation. Thus, one can speculate that CO would present "feedback control system," by generating ROS to signal preconditioning but also capable of limiting ROS generation by uncoupling mitochondria and avoiding further oxidative stress. Future investigation will be necessary to disclose this subject.

In conclusion, modulation of astrocytic metabolism appears as a novel and promising strategy to protect the brain against hypoxia-ischemia and reperfusion. Moreover, astrocytes are the most metabolic active cells in the CNS; and the importance of astrocytic metabolism modulation is not limited to its cell autonomous functioning but is also crucial for the maintenance of normal neuronal transmission and metabolism.

REFERENCES

1. Motterlini, R., and Otterbein, L. E. (2010) The therapeutic potential of carbon monoxide. *Nat. Rev. Drug Discov.* **9,** 728 –743
2. Soares, M. P., and Bach, F. H. (2009) Heme oxygenase-1: From biology to therapeutic potential. *Trends Mol. Med.* **15,** 50 –58
3. Bannenberg, G. L., and Vieira, H. L. (2009) Therapeutic applications of the gaseous mediators carbon monoxide and hydrogen sulfide. *Expert. Opin. Ther. Pat.* **19,** 663– 682
4. Ryter, S. W., Alam, J., and Choi, A. M. (2006) Heme oxygenase-1/carbon monoxide: From basic science to therapeutic applications. *Physiol. Rev.* **86,** 583– 650
5. Zhang, X., Shan, P., Alam, J., Davis, R. J., Flavell, R. A., and Lee, P. J. (2003) Carbon monoxide modulates Fas/Fas ligand, caspases, and Bcl-2 family proteins via the p38α mitogen-activated protein kinase pathway during ischemia-reperfusion lung injury. *J. Biol. Chem.* **278,** 22061–22070
6. Panahian, N., Yoshiura, M., and Maines, M. D. (1999) Overexpression of heme oxygenase-1 is neuroprotective in a model of permanent middle cerebral artery occlusion in transgenic mice. *J. Neurochem.* **72,** 1187–1203
7. Chora, A. A., Fontoura, P., Cunha, A., Pais, T. F., Cardoso, S., Ho, P. P., Lee, L. Y., Sobel, R. A., Steinman, L., and Soares, M. P. (2007) Heme oxygenase-1 and carbon monoxide suppress autoimmune neuroinflammation. *J. Clin. Invest.* **117,** 438 – 447
8. Zimmermann, A., Leffler, C. W., Tcheranova, D., Fedinec, A. L., and Parfenova, H. (2007) Cerebroprotective effects of the CO-releasing molecule CORM-A1 against seizure-induced neonatal vascular injury. *Am. J. Physiol. Heart Circ. Physiol.* **293,** H2501–2507
9. Queiroga, C. S., Almeida, A. S., Martel, C., Brenner, C., Alves, P. M., and Vieira, H. L. (2010) Glutathionylation of adenine nucleotide translocase induced by carbon monoxide prevents mitochondrial membrane permeabilization and apoptosis. *J. Biol. Chem.* **285,** 17077–17088
10. Vieira, H. L., Queiroga, C. S., and Alves, P. M. (2008) Preconditioning induced by carbon monoxide provides neuronal protection against Apoptosis. *J. Neurochem.* **107,** 375–384
11. Wang, B., Cao, W., Biswal, S., and Doré, S. (2011) Carbon monoxide-activated nrf2 pathway leads to protection against permanent focal cerebral ischemia. *Stroke* **42,** 2605–2610
12. Zeynalov, E., and Doré, S. (2009) Low doses of carbon monoxide protect against experimental focal brain ischemia. *Neurotox. Res.* **15,** 133–137
13. Tsui, T. Y., Obed, A., Siu, Y. T., Yet, S. F., Prantl, L., Schlitt, H. J., and Fan, S. T. (2007) Carbon monoxide inhalation rescues mice from fulminant hepatitis through improving hepatic energy metabolism. *Shock* **27,** 165–171
14. Tsui, T. Y., Siu, Y. T., Schlitt, H. J., and Fan, S. T. (2005) Heme oxygenase-1-derived carbon monoxide stimulates adenosine triphosphate generation in human hepatocyte. *Biochem. Biophys. Res. Commun.* **336,** 898 –902
15. Bilban, M., Haschemi, A., Wegiel, B., Chin, B. Y., Wagner, O., and Otterbein, L. E. (2008) Heme oxygenase and carbon monoxide initiate homeostatic signaling. *J. Mol. Med.* **86,** 267–279
16. D'Amico, G., Lam, F., Hagen, T., and Moncada, S. (2006) Inhibition of cellular respiration by endogenously produced carbon monoxide. *J. Cell Sci.* **119,** 2291–2298
17. Taillé, C., El-Benna, J., Lanone, S., Boczkowski, J., and Motterlini, R. (2005) Mitochondrial respiratory chain and NAD(P)H oxidase are targets for the

antiproliferative effect of carbon monoxide in human airway smooth muscle. *J. Biol. Chem.* **280,** 25350–25360

18. Zuckerbraun, B. S., Chin, B. Y., Bilban, M., d'Avila, J. C., Rao, J., Billiar, T. R., and Otterbein, L. E. (2007) Carbon monoxide signals via inhibition of cytochrome c oxidase and generation of mitochondrial reactive oxygen species. *FASEB J.* **21,** 1099–1106

19. Suliman, H. B., Carraway, M. S., Tatro, L. G., and Piantadosi, C. A. (2007) A new activating role for CO in cardiac mitochondrial biogenesis. *J. Cell Sci.* **120,** 299–308

20. Suliman, H. B., Carraway, M. S., Ali, A. S., Reynolds, C. M., Welty-Wolf, K. E., and Piantadosi, C. A. (2007) The CO/HO system reverses inhibition of mitochondrial biogenesis and prevents murine doxorubicin cardiomyopathy. *J. Clin. Invest.* **117,** 3730–3741

21. Dirnagl, U., Becker, K., and Meisel, A. (2009) Preconditioning and tolerance against cerebral ischaemia: From experimental strategies to clinical use. *Lancet Neurol.* **8,** 398–412

22. Vannucci, S. J., and Hagberg, H. (2004) Hypoxia-ischemia in the immature brain. *J. Exp. Biol.* **207,** 3149–3154

23. McCarthy, K. D., and de Vellis, J. (1980) Preparation of separate astroglial and oligodendroglial cell cultures from rat cerebral tissue. *J. Cell Biol.* **85,** 890–902

24. Sá Santos, S., Fonseca, L. L., Monteiro, M. A., Carrondo, M. J., and Alves, P. M. (2005) Culturing primary brain astrocytes under fully controlled environment in a novel bioreactor. *J. Neurosci. Res.* **79,** 26–32

25. Atkinson, B., and Mavituna, F. (1987). *Biochemical Engineering Fundamentals*, McGraw-Hill, Inc., New York

26. Kristián, T., Gertsch, J., Bates, T. E., and Siesjö, B. K. (2000) Characteristics of the calcium-triggered mitochondrial permeability transition in nonsynaptic brain mitochondria: effect of cyclosporin A and ubiquinone O. *J. Neurochem.* **74,** 1999–2009

27. Sims, N. R. (1990) Rapid isolation of metabolically active mitochondria from rat brain and subregions using Percoll density gradient centrifugation. *J. Neurochem.* **55,** 698–707

28. Maranga, L., and Goochee, C. F. (2006) Metabolism of PER. C6 cells cultivated under fed-batch conditions at low glucose and glutamine levels. *Biotechnol. Bioeng.* **94,** 139–150

29. Alonso, J. R., Cardellach, F., López, S., Casademont, J., and Miró, O. (2003) Carbon monoxide specifically inhibits cytochrome *c* oxidase of human mitochondrial respiratory chain. *Pharmacol. Toxicol.* **93,** 142–146

30. Queiroga, C. S., Almeida, A. S., Alves, P. M., Brenner, C., and Vieira, H. L. (2011) Carbon monoxide prevents hepatic mitochondrial membrane permeabilization. *BMC Cell Biol.* **12,** 10

31. Chen, Z. X., and Pervaiz, S. (2007) Bcl-2 induces pro-oxidant state by engaging mitochondrial respiration in tumor cells. *Cell Death Differ.* **14,** 1617–1627

32. Chen, Z. X., and Pervaiz, S. (2010) Involvement of cytochrome *c* oxidase subunits Va and Vb in the regulation of cancer cell metabolism by Bcl-2. *Cell Death Differ.* **17,** 408–420

33. Chin, B. Y., Jiang, G., Wegiel, B., Wang, H. J., Macdonald, T., Zhang, X. C., Gallo, D., Cszimadia, E., Bach, F. H., Lee, P. J., and Otterbein, L. E. (2007) Hypoxia-inducible factor 1α stabilization by carbon monoxide results in cytoprotective preconditioning. *Proc. Natl. Acad. Sci. U.S.A.* **104,** 5109–5114

34. Stein, A. B., Guo, Y., Tan, W., Wu, W. J., Zhu, X., Li, Q., Luo, C., Dawn, B., Johnson, T. R., Motterlini, R., and Bolli, R. (2005) Administration of a CO-releasing molecule induces late preconditioning against myocardial infarction. *J. Mol. Cell Cardiol.* **38,** 127–134

35. Vannucci, R. C., Towfighi, J., and Vannucci, S. J. (1998) Hypoxic preconditioning and hypoxic-ischemic brain damage in the immature rat: Pathologic and metabolic correlates. *J. Neurochem.* **71,** 1215–1220

36. Ahlstrom, K., Biber, B., Aberg, A., Waldenstrom, A., Ronquist, G., Abrahamsson, P., Stranden, P., Johansson, G., and Haney, M. F. (2009) Metabolic responses in ischemic myocardium after inhalation of carbon monoxide. *Acta Anesthesiol. Scand.* **53,** 1036–1042

37. Fukuda, R., Zhang, H., Kim, J. W., Shimoda, L., Dang, C. V., and Semenza, G. L. (2007) HIF-1 regulates cytochrome oxidase subunits to optimize efficiency of respiration in hypoxic cells. *Cell* **129,** 111–122

38. Di Noia, M. A., Van Driesche, S., Palmieri, F., Yang, L. M., Quan, S., Goodman, A. I., and Abraham, N. G. (2006) Heme oxygenase-1 enhances renal mitochondrial transport carriers and cytochrome *c* oxidase activity in experimental diabetes. *J. Biol. Chem.* **281,** 15687–15693

39. Lo Iacono, L., Boczkowski, J., Zini, R., Salouage, I., Berdeaux, A., Motterlini, R., and Morin, D. (2011) A carbon monoxide-releasing molecule (CORM-3) uncouples mitochondrial respiration and modulates the production of reactive oxygen species. *Free Radic. Biol. Med.* **50,** 1556–1564

40. Motterlini, R., Clark, J. E., Roresti, R., Sarathchandra, P., Mann, B. E., and Grenn, C. J. (2002) Carbon monoxide-releasing molecules: characterization of biochemical and vascular activites. *Circ. Res.* **90,** E17–E24